

Confined hydrogen atom by the Lagrange-mesh method: Energies, mean radii, and dynamic polarizabilities

D. Baye^{1,2,*} and K. D. Sen^{3,†}¹*Physique Quantique, C.P. 165/82, Université Libre de Bruxelles, B 1050 Brussels, Belgium*²*Physique Nucléaire Théorique et Physique Mathématique, C.P. 229, Université Libre de Bruxelles, B 1050 Brussels, Belgium*³*School of Chemistry, University of Hyderabad, Hyderabad 500046, India*

(Received 26 May 2008; published 5 August 2008)

The Lagrange-mesh method is an approximate variational calculation which resembles a mesh calculation because of the use of a Gauss quadrature. The hydrogen atom confined in a sphere is studied with Lagrange-Legendre basis functions vanishing at the center and surface of the sphere. For various confinement radii, accurate energies and mean radii are obtained with small numbers of mesh points, as well as dynamic dipole polarizabilities. The wave functions satisfy the cusp condition with 11-digit accuracy.

DOI: [10.1103/PhysRevE.78.026701](https://doi.org/10.1103/PhysRevE.78.026701)

PACS number(s): 02.70.Hm, 02.70.Jn, 31.15.ap

I. INTRODUCTION

Recent developments in nanotechnology have renewed interest in the modeling of spatially confined quantum systems under the influence of a wide variety of confining potentials. For example, the electronic properties of quantum dots are studied by considering a set of electrons confined within a prescribed potential. Atoms and molecules confined inside helium droplets, fullerenes, and zeolites provide further possibilities of constructing spatially confined systems. For a detailed account of such applications we refer the reader to recent review articles [1–3] and references therein.

The hydrogen atom confined in an impenetrable sphere was introduced to simulate the effect of high pressure on its static dipole polarizability [4]. An analytical solution in terms of the confluent hypergeometric function exists, but the energies are only implicitly given [5,6]. The spectrum of this system is discrete, without the accidental degeneracy of the free hydrogen atom. In spite of this lack of degeneracy, the levels of the confined hydrogen atom are labeled with the same quantum numbers nl as for free hydrogen, where $n-l-1$ represents the number of nodes of the radial wave function.

Two kinds of degeneracies are identified for the confined states [7–10]. They appear for special values of the radius R of spherical confinement, corresponding to the locations of the radial nodes in the free hydrogen atom states with quantum numbers nl . For these values, the Schrödinger equation and the boundary condition are simultaneously satisfied at the same energy as for the free atom. The confined wave function has one node less than the free one. This *incidental degeneracy* implies that the energy of a confined nl state equals that of the free $n+1, l$ state. For example, at $R=2$ a.u., the confined $1s$ state has the same energy as the $2s$ state of the free H atom. Other examples of incidental degeneracy have been discussed in the literature [11]. The *simultaneous degeneracy* arises at the values $R=(l+1)(l+2)$ and is such that a pair of confined states with quantum numbers nl

and $n+1, l+2$ correspond to the same energy value [7]. For example, at $R=2$ a.u., the $(2s, 3d), (3s, 4d), \dots$ pairs become degenerate, with different energy values for each pair.

We note here that except for the incidental degeneracy cases, the energy of the confined state is not analytically known. A numerical resolution is thus necessary [12]. This problem is a good testing ground for numerical methods because the energies in Ref. [12] can be considered as exact. In this paper we apply the Lagrange-mesh method to such confined model calculations.

The Lagrange-mesh method is an approximate variational calculation which resembles a mesh calculation because of the use of a Gauss quadrature [13–16]. It provides very accurate results with few mesh points in a variety of quantum-mechanical problems: bound [17] and scattering [18] states, three-body atomic [19] and nuclear [20] systems, etc. Strikingly, its accuracy is not worse than the accuracy of the corresponding variational calculation, performed without Gauss approximation [15]. This accuracy on energies, radii, and several other observables is much better than the accuracy of the Gauss quadrature on matrix elements between Lagrange functions. For example, while scalar products of different Lagrange functions seem to vanish when calculated with the Gauss quadrature, they do not vanish when calculated exactly. Nevertheless, the Lagrange basis functions can be treated as an orthogonal basis without loss of accuracy.

This method has, however, the same limitations as the Gauss quadrature; i.e., the accuracy disappears if the integrands or some of their derivatives have discontinuities. The first attempts to calculate with this technique the energies of the simple hydrogen atom failed because of the singularity at the origin in the Coulomb potential for s waves and in the centrifugal and Coulomb terms for other partial waves [13]. The problem could be cured with the regularization technique [14–16]: the basis functions are multiplied by some factors aimed at removing discontinuities of the integrands while preserving the advantages of the Gauss quadrature. With this approach, the test with the hydrogen atom becomes successful.

As stated above, our aim is to apply this simple technique to the hydrogen atom confined in a spherical box. The basis functions must thus vanish at the surface of the sphere. For

*dbaye@ulb.ac.be

†kalidas.sen@gmail.com

the unconfined hydrogen atom, accurate solutions with few mesh points are obtained with a regularized Lagrange-Laguerre basis [14–16,21]. Here we introduce a Lagrange mesh, based on shifted Legendre polynomials multiplied by a regularization factor, that ensures that the basis functions vanish at the origin and at the boundary. The resulting simple mesh equations are used to compute the energies, mean radii, and dynamic dipole polarizabilities [22,23].

For the polarizabilities, the Lagrange-mesh technique can be compared with the mapped Fourier grid method of Refs. [23,24]. Basically, that approach is based on the discrete variable representation (DVR) [25] and very close to a Lagrange-mesh method making use of a mapped sinc basis [16]. This comparison will allow us to clarify differences between these approaches.

In Sec. II, we summarize the Lagrange-mesh method and introduce a Lagrange basis. In Sec. III, we present and discuss the results. Section IV contains concluding remarks.

II. CONFINED HYDROGEN ON A LAGRANGE MESH

A. Lagrange basis and Lagrange mesh

A Lagrange basis is a set of N functions f_i associated with a Lagrange mesh of N points Rx_i ($i=1, N$) on the interval $[0, R]$ [13–16]. With a simple scaling, it is thus sufficient to study the problem on $[0, 1]$.

The Lagrange functions are N orthonormal functions $f_i(x)$ verifying at the N mesh points $x_i \in [0, 1]$ the Lagrange conditions

$$f_i(x_j) = \lambda_i^{-1/2} \delta_{ij}; \quad (1)$$

i.e., each function $f_i(x)$ vanishes at all mesh points except at x_i . The coefficients λ_i are the weights associated with a Gauss quadrature approximation for the $[0, 1]$ interval

$$\int_0^1 g(x) dx \approx \sum_{i=1}^N \lambda_i g(x_i). \quad (2)$$

Conditions (1) and (2) are realized when the x_i are zeros of the shifted Legendre polynomial $P_N(2x-1)$, i.e.,

$$P_N(2x_i - 1) = 0. \quad (3)$$

Quadrature (2) is then exact for any polynomial with degree not larger than $2N-1$ [26]. Lagrange-Legendre functions are continuous and indefinitely differentiable anywhere and read

$$\hat{f}_i(x) = (-1)^{i+N} \frac{P_N(2x-1)}{\sqrt{x_i(1-x_i)}(x-x_i)}. \quad (4)$$

They are polynomials of degree $N-1$. They form a variational basis equivalent to the Legendre basis $P_0(2x-1)$ to $P_{N-1}(2x-1)$. The weights λ_i are equal to the traditional Gauss-Legendre weights for the $[-1, +1]$ interval [27], divided by 2. In most of the following, neither the explicit expression of the Lagrange functions nor the weights will be needed.

The Lagrange functions (4) are not regularized at the origin and are thus not efficient for the Coulomb problem or in

the presence of a centrifugal barrier. Moreover, they do not vanish at $x=1$ and are thus not practical for confined problems. Hence we replace them by

$$f_i(x) = \frac{x(1-x)}{x_i(1-x_i)} \hat{f}_i(x). \quad (5)$$

The functions f_i are polynomials of degree $N+1$ that vanish at 0 and 1. They still have the Lagrange property (1). Notice that the same properties for the Lagrange functions, but associated with a different mesh, can be obtained from the Jacobi polynomial $P_N^{(2,2)}$ [27] multiplied by the square root of its weight function. However, the Coulomb and centrifugal terms would be more difficult to handle [28].

Contrary to the functions (4), the Lagrange functions (5) are not orthogonal, but because of the Lagrange conditions (1), they are approximately orthogonal at the Gauss approximation (2),

$$\int_0^1 f_i(x) f_j(x) dx \approx \delta_{ij}. \quad (6)$$

The Gauss quadrature is not exact because the degree $2N+2$ of the integrand exceeds $2N-1$. In the following, we shall calculate all integrals with the Gauss quadrature and thus treat the basis as an orthonormal basis. Although the Gauss quadrature is exact for none of the integrals, this approximation will prove very accurate.

B. Energies and radii

For a partial wave l , the Schrödinger equation of an electron confined over the domain $[0, R]$ and submitted to a central potential $V(r)$ can be written as

$$H_l \psi_l(r) = E \psi_l(r), \quad (7)$$

where the Hamiltonian reads in atomic units

$$H_l = -\frac{1}{2} \frac{d^2}{dr^2} + \frac{l(l+1)}{2r^2} + V(r). \quad (8)$$

The partial wave function is approximated as

$$\psi_l(r) = R^{-1/2} \sum_{j=1}^N c_{lj} f_j(r/R). \quad (9)$$

From property (1), one deduces $c_{lj} \approx (R\lambda_j)^{1/2} \psi_l(Rx_j)$.

With property (1), the matrix elements of operator $-d^2/dx^2$ can be computed with the Gauss-Legendre approximation (2) on the $[0, 1]$ interval with

$$T_{ij} = -\langle f_i | \frac{d^2}{dx^2} | f_j \rangle \approx -\lambda_i^{1/2} f_j''(x_i). \quad (10)$$

The second derivative of (5) provides the simple expressions

$$T_{ij} = (-1)^{i+j} [x_i(1-x_i)x_j(1-x_j)]^{-1/2} \frac{x_i + x_j - 2x_i x_j}{(x_i - x_j)^2} \quad (11)$$

for $i \neq j$ and

$$T_{ii} = \frac{1}{3x_i(1-x_i)} \left[N(N+1) + \frac{1}{x_i(1-x_i)} \right] \quad (12)$$

for $i=j$. Notice that the Gauss approximation is not exact here since the degree of the integrand is one unit larger than $2N-1$. But the result of the Gauss quadrature is symmetrical, in agreement with Hermiticity. Otherwise, a more elaborate calculation would have been necessary [17].

On this Lagrange mesh, the Schrödinger equation (7) becomes [13–16]

$$\sum_{j=1}^N [H_{lij} - E\delta_{ij}]c_{lj} = 0, \quad (13)$$

with the Hamiltonian matrix elements

$$H_{lij} = \frac{1}{2R^2} \left[T_{ij} + \frac{l(l+1)}{x_i^2} \delta_{ij} \right] + V(Rx_i) \delta_{ij}. \quad (14)$$

Equation (13) provides the energies and the coefficients c_{lj} . As mentioned above, these coefficients are related to the values of the wave function at mesh points. Nevertheless, contrary to finite differences or other mesh methods, these coefficients also provide values of the wave function (9) everywhere.

Matrix elements of local operators can also be calculated easily with the Gauss quadrature (2) and property (1). For $k \geq -2$, one has

$$\langle f_i | x^k | f_j \rangle \approx x_j^k \delta_{ij}. \quad (15)$$

The particular case $k=0$ is nothing but (6). Hence mean values of r^k are given by

$$\langle r^k \rangle \approx R^k \sum_{j=1}^N c_{lj}^2 x_j^k \quad (16)$$

for $k \geq -2$. Although expression (16) is not exact, we shall see that it provides very accurate values with small numbers of mesh points.

C. Dynamical dipole polarizabilities

With the Dalgarno-Lewis method [29], the dynamical dipole polarizability of state lm is given by

$$\alpha_{lm}(\omega) = \sum_{l'} C_{lm l'} \int_0^R \psi_{l'}(r) r [\psi_{l'm+}^{(1)}(r) + \psi_{l'm-}^{(1)}(r)] dr, \quad (17)$$

where the zeroth-order wave function $\psi_{l'}$ is a solution of (7). The coefficients read

$$C_{lm l'} = (-1)^m (2l+1)^{1/2} (2l'+1)^{1/2} \begin{pmatrix} l' & 1 & l \\ -m & 0 & m \end{pmatrix} \begin{pmatrix} l' & 1 & l \\ 0 & 0 & 0 \end{pmatrix}. \quad (18)$$

The sum in (17) is thus restricted to $l' = |l \pm 1|$ and $l' \geq |m|$. The functions $\psi_{l'm\pm}^{(1)}$ are solutions of the inhomogeneous radial equations

$$(H_{l'} - E \pm \omega) \psi_{l'm\pm}^{(1)}(r) = -C_{lm l'} r \psi_{l'}(r), \quad (19)$$

which vanish at 0 and R .

We now expand the first-order functions as

$$\psi_{l'm\pm}^{(1)}(r) = R^{-1/2} \sum_{j=1}^N c_{l'm\pm,j}^{(1)} f_j(r/R). \quad (20)$$

At the Gauss approximation, Eq. (19) leads to the algebraic system

$$\sum_{j=1}^N [H_{l'ij} - (E \mp \omega) \delta_{ij}] c_{l'm\pm,j}^{(1)} = -C_{lm l'} R x_i c_{li} \quad (21)$$

and Eq. (17) provides the polarizabilities

$$\alpha_{lm}(\omega) = R \sum_{l'} C_{lm l'} \sum_{j=1}^N c_{lj} x_j (c_{l'm+j}^{(1)} + c_{l'm-j}^{(1)}). \quad (22)$$

TABLE I. Convergence of energies E and mean radii of the ground state of the confined hydrogen atom for $R=2$ and 10 as a function of the number N of mesh points. The last column corresponds to the cusp condition (25). Exact results are rounded from Ref. [12].

N	E	$\langle 1/r \rangle$	$\langle r \rangle$	$\langle r^2 \rangle$	$\rho'(0)/\rho(0)$
$R=2$					
4	-0.125061	1.53624	0.8609	0.8729	-1.9945
6	-0.1250000014	1.535161756	0.85935332	0.8748247	-1.999974
8	-0.12500000000003	1.53516170643364	0.8593531742681	0.87482539412421	-1.999999946
10	-0.125000000000001	1.53516170643331	0.85935317426677	0.87482539413417	-1.99999999939
ex.	-0.125000000000000	1.53516170643330	0.85935317426677	0.87482539413417	-2
$R=10$					
10	-0.5000016	1.0000463	1.50000626	2.99931	-1.99805
15	-0.49999926328191	1.000011692830	1.49993637881	2.99945950866	-1.9999920
20	-0.49999926328153	1.00001169282110	1.49993637877150	2.9994595088658	-1.99999999944
25	-0.49999926328148	1.00001169282098	1.49993637877163	2.9994595088663	-1.99999999996
ex.	-0.49999926328153	1.00001169282108	1.49993637877151	2.9994595088658	-2

TABLE II. Energies E and average radii of the confined hydrogen atom for $R=2$ with $N=20$ mesh points: (a) present work and (b) exact results from Ref. [12], except for the $2p$ state where the average radii are from Ref. [30].

nl		E	$\langle 1/r \rangle$	$\langle r \rangle$	$\langle r^2 \rangle$
1s	(a)	-0.1250000000000	1.5351617064333	0.8593531742668	0.8748253941342
	(b)	-0.1250000000000	1.53516170643330	0.85935317426677	0.87482539413417
2s	(a)	3.3275091564964	1.6462701389774	1.0219789235879	1.3320904586151
	(b)	3.32750915649647	1.64627013897734	1.02197892358789	1.33209045861518
3s	(a)	9.3141504354036	1.8141208485472	1.0168625603981	1.3453611004185
	(b)	9.31415043540360			
2p	(a)	1.5760187856062	0.97234328360280	1.14107908207279	1.4056651407853
	(b)	1.57601878560634	0.97234328		1.405663
3p	(a)	6.2690027919866	1.20705920187634	1.07290780001893	1.3855398769833
	(b)	6.26900279198648			
4p	(a)	13.510584159771	1.36369836877412	1.04542352584587	1.3669819628524
3d	(a)	3.3275091564964	0.83295185750304	1.27525204948509	1.7067631688822
	(b)	3.32750915649647			
4d	(a)	9.3141504354037	1.03301318210024	1.14129322618607	1.4930470696061
	(b)	9.31415043540360			
5d	(a)	17.8160934959697	1.17178541254853	1.08944558050605	1.4244486476031
	(b)	17.81609349596967			

III. RESULTS AND DISCUSSION

A. Energies and mean radii

Equation (19) provides energies for an arbitrary potential V . In particular, one can test the correctness of the code with $V=0$. From now on, we choose the Coulomb potential $V=-1/r$.

With the Lagrange-mesh technique, we calculate the energies of system (13) for some values of the confinement radius R . The convergence is very fast as illustrated by Table I. At $R=2$, the ground-state energy is exactly $E=-1/8$ because of the incidental degeneracy. One observes that the convergence is exponential: excellent results are already

obtained with only eight points. With $N=10$, the energy is not improved because of rounding errors, but the wave function becomes more accurate as shown by the better agreement with the cusp condition defined below in Eq. (25). By extrapolation, a 100-digit accuracy such as in Ref. [12] will be reached with less than 50 mesh points in a multiprecision calculation. For $R=10$, the energy does not differ much from the free-hydrogen value $-1/2$. Here also the convergence is exponential but with some delay. One observes that larger rounding errors make $N=25$ slightly less good than $N=20$.

The accuracy of the results in the following tables is checked by comparing the results obtained with the mentioned number N of points with results obtained with $N+4$ and $N+10$ points and by only keeping stable digits. All digits

TABLE III. Energies E and mean radii of the confined hydrogen atom for $R=20$: (a) present work with $N=40$ and (b) Ref. [12]; (c) comparison with free hydrogen.

nl		E	$\langle 1/r \rangle$	$\langle r \rangle$	$\langle r^2 \rangle$
1s	(a)	-0.4999999999992	1.0000000000012	1.499999999977	2.999999999640
	(b)	-0.4999999999999	1.0000000000023	1.499999999757	2.999999999637
	(c)	-0.5	1	1.5	3
2s	(a)	-0.12498711431291	0.25017311811489	5.9926621769945	41.849320843821
	(b)	-0.12498711431292	0.25017311811490	5.9926621769942	41.849320843817
	(c)	-0.125	0.25	6	42
2p	(a)	-0.12499460664707	0.25007388596077	4.9965331340246	29.933020319372
	(b)	-0.12499460664708			
	(c)	-0.125	0.25	5	30
3p	(a)	-0.05161141976110	0.13021802735253	10.654910283762	129.09441512402
	(c)	-0.0555555555555	0.1111111111111	12.5	180

TABLE IV. Density and its first and second derivatives at the origin. The last column is a test of the cusp condition and should be compared with -2 .

nl	$\rho(0)$	$\rho'(0)$	$\rho''(0)$	$\rho'(0)/\rho(0)$
$R=2$ ($N=20$)				
1s	9.496131945033	-18.9922638902	33.23646179	-2.000000000010
2s	20.679450381857	-41.3589007639	-22.81657942	-2.000000000010
3s	37.81519138482	-75.630382772	-343.5712035	-2.000000000060
$R=20$ ($N=40$)				
1s	4.000000000000	-7.99999999993	16.000000004	-1.99999999998
2s	0.5005342706145	-1.00106854122	1.751861348	-1.99999999998
3s	0.2221433387561	-0.44428667751	0.755263078	-1.99999999998

of the presented results, except the last one, are expected to be correct.

Results obtained with $N=20$ at $R=2$ for various states are displayed in Table II. For s states, they are compared with the (truncated) 100-digit results of Ref. [12], when available. The agreement is excellent both for energies and mean radii. For d states, a comparison with the exact energies of Ref. [12] is also possible because of the simultaneous degeneracy property [7], valid at $R=2$, $E_{nd}=E_{(n-1)s}$. Such a property does not exist for mean radii.

For p states, the agreement is also excellent for the energies. However, mean radii in Ref. [12] are completely different from ours for the $2p$ state (not shown in the table). We note here that our results agree well with those reported in Table IV of the earlier Ref. [30], though using a less accurate method than in Ref. [12]. We think that the values in Ref. [12] are incorrect because, at $R=20$, they do not seem to tend towards the free-hydrogen values $\langle 1/r \rangle = 1/n^2$, $\langle r \rangle = \frac{1}{2}[3n^2 - l(l+1)]$, and $\langle r^2 \rangle = \frac{1}{2}n^2[5n^2 + 1 - 3l(l+1)]$, while our results have this behavior as shown in Table III. The results for the confined atom are very close to those for the free atom as long as the free-hydrogen density distribution is negligible beyond R .

The Lagrange-mesh method also provides approximate wave functions. To illustrate this point, we present in Table IV values of the $l=0$ radial density $\rho(r) = r^{-2}|\psi_0(r)|^2$ and of

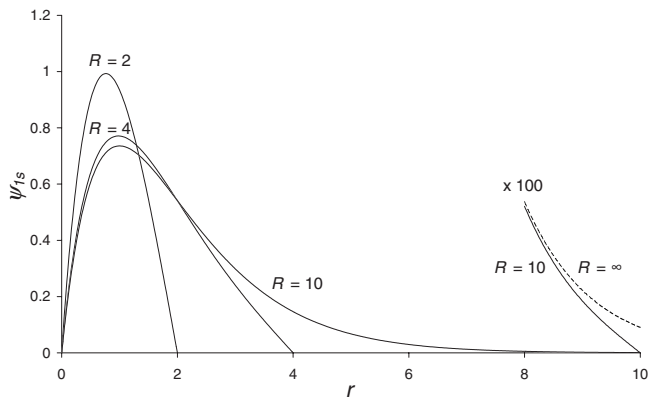


FIG. 1. Radial wave functions of the 1s state for confinement radii $R=2, 4$, and 10 ($N=20$). The free-hydrogen wave function $2r \exp(-r)$ (dashed line) is not distinct from $R=10$ except beyond $r=8$ (see enlargement).

its derivatives at the origin. This allows us to test the cusp condition. The values of the radial function $r^{-1}\psi_0(r)$ and of its first derivative at the origin can be obtained from Eq. (9) with

$$[x^{-1}f_i(x)]_{x=0} = \frac{(-1)^{i+1}}{\sqrt{x_i^3(1-x_i)}} \quad (23)$$

and

$$[x^{-1}f_i(x)]'_{x=0} = \frac{(-1)^{i+1}}{\sqrt{x_i^3(1-x_i)}} \left[\frac{1}{x_i} - 1 - N(N+1) \right]. \quad (24)$$

The cusp condition reads

$$\frac{\rho'(0)}{\rho(0)} = 2 \frac{[r^{-1}\psi_0(r)]'_{r=0}}{[r^{-1}\psi_0(r)]_{r=0}} = -2. \quad (25)$$

This condition is accurately verified in Table IV. The s -state densities at the origin are related to the corresponding energies by [31]

$$\frac{\rho''(0)}{\rho(0)} = \frac{2}{3}(5 - 2E). \quad (26)$$

The values in Tables III and IV satisfy this relation with an accuracy of about 10^{-9} . Together with the cusp condition,

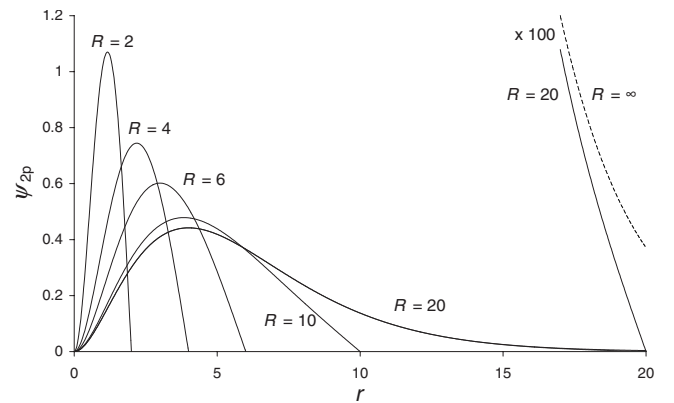


FIG. 2. Radial wave functions of the 2p state for confinement radii $R=2, 4, 6, 10$, and 20 ($N=30$). The free-hydrogen wave function $(2\sqrt{6})^{-1}r^2 \exp(-r/2)$ (dashed line) is not distinct from $R=20$ except beyond $r=14$ (see enlargement).

TABLE V. Polarizabilities of the confined hydrogen atom for $R=2$ ($N=20$) and $R=10$ ($N=40$) compared with those of Ref. [23].

ω	$R=2$		$R=10$	
	Present	Ref. [23]	Present	Ref. [23]
<i>1s</i>				
0.0	0.3425581085153	0.3425581	4.496814184183	4.4968141
0.1	0.3437459741796	0.3437461	4.779924526766	4.7799245
0.2	0.3473595257444	0.3473595	5.928772212858	5.9287722
0.3	0.3535539725849	0.3535540	10.41075054702	10.410751
0.4	0.3626069110167	0.3626069	-31.2528276234	-31.252828
0.5	0.3749509012352	0.3749510	0.68698967794	0.68698974
<i>2s</i>				
0.0	-0.01688502110107	-0.0168851	-2086.463707870	-2086.4632
0.1	-0.01732626730118	-0.0173261	67.7669505903	67.766946
0.2	-0.01867291924822	-0.0186729	-67.9247444019	-67.924739
0.3	-0.02099621871629	-0.0209962	-13.63828233385	-13.638282
0.4	-0.02442373597004	-0.0244238	-4.323822661405	-4.3238212
0.5	-0.02915451224545	-0.0291545	-4.750719913081	-4.7507198
<i>2p0</i>				
0.0	0.28448371568205	0.2844837	2225.23860937	2225.2360
0.1	0.28534355414763	0.2853446	506.5517461982	506.55175
0.2	0.28795426767542	0.2879543	-34.22089537855	-34.220931
0.3	0.29241228096500	0.2924123	-25.45256476453	-25.452573
0.4	0.29888821566397	0.2988883	23.0002497144	23.000197
0.5	0.30764356928693	0.3076435	-1.534147279037	-1.5341475
<i>2p1</i>				
0.0	0.32018063185679	0.3201806	77.36538569235	77.365386
0.1	0.32122708494795	0.3212271	386.7864666270	386.78648
0.2	0.32440791787571	0.3244079	-34.582334518694	-34.582334
0.3	0.32985172999564	0.3298517	-10.486944612444	-10.486944
0.4	0.33778758626293	0.3377876	-6.9306779219840	-6.9306779
0.5	0.34857018983051	0.3485702	-4.1607660041581	-4.1607660

this confirms the accuracy of the s wave functions near the origin. At large R , the density at the origin and its derivatives are very close to the free-hydrogen values for the $1s$ state.

The wave function ψ_{1s} is displayed in Fig. 1 for several values of the confinement radius R . For $R=10$, the confined wave function is hardly distinguishable from the free-hydrogen one. At small r values, the confined wave function is slightly larger to ensure normalization to unity. They share five common digits between $r=2$ and $r=4$. Beyond $r=4$, the unconfined wave function is slightly larger. For r values around 6, the difference is about 0.1%. At $r=8$, it reaches 3%. Beyond this value, the two functions behave quite differently.

The wave function ψ_{2p} displayed in Fig. 2 shows a similar behavior. The $R=10$ confined wave function is now different from the free-hydrogen one because the free-hydrogen wave function is still large at $r=10$. For $R=20$, the confined and unconfined wave functions are very close up to $r=14$ where the difference becomes larger than 1%.

B. Dynamic dipole polarizabilities

Polarizabilities calculated with the Lagrange-mesh technique are displayed in Table V. They agree with the accurate results of Ref. [23] and improve them in spite of a much smaller number of mesh points. At $\omega=0$, they also agree with the values of Ref. [22].

It is interesting to compare the present method and the mapped Fourier grid method [23,24]. The latter method has been derived [24] in the spirit of the DVR [25]. As mentioned in Ref. [24], several expressions for the discrete kinetic-energy matrix elements T_{ij} provide essentially identical results. However, in the spirit of the Lagrange-mesh method, these kinetic-energy matrix elements correspond to three different Lagrange bases: Lagrange-Fourier [13,16], Lagrange-sinc [16,32], and parity-projected Lagrange-sinc. A parity-projected Lagrange-Fourier basis could also have been used [21].

Since both methods are so close, where do the differences of accuracy and of number of mesh points come from? Con-

trary to the present method, the mapped Fourier grid method does not regularize the singularity of the Coulomb potential and of the centrifugal term. The accuracy of the Gauss-Fourier [16] approximation hidden in the Fourier grid method is restricted by this singularity and higher numbers of mesh points need be used.

IV. CONCLUSIONS

The Lagrange-mesh approximation provides very accurate energies and wave functions of the confined hydrogen atom with small numbers of mesh points. The high accuracy reached requires the use of a regularization of the Coulomb and centrifugal singularity at the origin. This is the main difference with the mapped Fourier grid method of Refs. [23,24] which requires many more mesh points. We did not

attempt to reach the accuracy of the 100-digit results of Ref. [12]. However, with multiprecision arithmetics, the accuracy of the Lagrange-mesh method can still become much better.

The simplicity of the method allows fast and accurate calculations of various properties of the atom such as mean radii, densities, etc. In particular, the Lagrange-mesh method has been found efficient to calculate highly accurate dynamical polarizabilities in this simple problem. It would thus be interesting to apply it to the calculation of polarizabilities of three-body atomic or molecular Coulomb systems.

ACKNOWLEDGMENTS

This text presents research results of the Belgian Program No. P6/23 on interuniversity attraction poles initiated by the Belgian-state Federal Services for Scientific, Technical and Cultural Affairs (FSTC).

-
- [1] W. Jaskolski, Phys. Rep. **271**, 1 (1996).
 - [2] A. L. Buchachenko, J. Phys. Chem. B **105**, 5839 (2001).
 - [3] V. K. Dolmatov, A. S. Baltentkov, J.-P. Connerade, and S. T. Manson, Radiat. Phys. Chem. **70**, 417 (2004).
 - [4] A. Michels, J. de Boer, and A. Bijl, Physica (Amsterdam) **4**, 981 (1937).
 - [5] A. Sommerfeld and H. Welker, Ann. Phys. **32**, 56 (1938).
 - [6] E. Ley-Koo and S. Rubinstein, J. Chem. Phys. **71**, 351 (1979).
 - [7] V. I. Pupyshev and A. V. Scherbinin, Chem. Phys. Lett. **295**, 217 (1998).
 - [8] V. I. Pupyshev and A. V. Scherbinin, Phys. Lett. A **299**, 371 (2002).
 - [9] S. Goldman and C. Joslin, J. Phys. Chem. **96**, 6021 (1992).
 - [10] B. L. Burrows and M. Cohen, Phys. Rev. A **72**, 032508 (2005).
 - [11] K. D. Sen, J. Chem. Phys. **122**, 194324 (2005).
 - [12] N. Aquino, G. Campoy, and H. E. Montgomery, Jr., Int. J. Quantum Chem. **107**, 1548 (2007).
 - [13] D. Baye and P.-H. Heenen, J. Phys. A **19**, 2041 (1986).
 - [14] M. Vincke, L. Malegat, and D. Baye, J. Phys. B **26**, 811 (1993).
 - [15] D. Baye, M. Hesse, and M. Vincke, Phys. Rev. E **65**, 026701 (2002).
 - [16] D. Baye, Phys. Status Solidi B **243**, 1095 (2006).
 - [17] D. Baye, M. Vincke, and M. Hesse, J. Phys. B **41**, 055005 (2008).
 - [18] M. Hesse, J.-M. Sparenberg, F. Van Raemdonck, and D. Baye, Nucl. Phys. A **640**, 37 (1998).
 - [19] M. Hesse and D. Baye, J. Phys. B **32**, 5605 (1999); **34**, 1425 (2001); **36**, 139 (2003).
 - [20] P. Descouvemont, C. Daniel, and D. Baye, Phys. Rev. C **67**, 044309 (2003).
 - [21] D. Baye, J. Phys. B **28**, 4399 (1995).
 - [22] H. E. Montgomery, Jr., Chem. Phys. Lett. **352**, 529 (2002).
 - [23] S. Cohen, S. I. Themelis, and K. D. Sen, Int. J. Quantum Chem. **108**, 351 (2008).
 - [24] S. Cohen and S. I. Themelis, J. Chem. Phys. **124**, 134106 (2006).
 - [25] J. C. Light, I. P. Hamilton, and J. V. Lill, J. Chem. Phys. **82**, 1400 (1985).
 - [26] G. Szegő, *Orthogonal Polynomials* (American Mathematical Society, Providence, RI, 1967).
 - [27] *Handbook of Mathematical Functions*, edited by M. Abramowitz and I. A. Stegun (Dover, New York, 1970).
 - [28] D. Baye, M. Hesse, J.-M. Sparenberg, and M. Vincke, J. Phys. B **31**, 3439 (1998).
 - [29] A. Dalgarno and J. T. Lewis, Proc. R. Soc. London, Ser. A **233**, 70 (1955).
 - [30] N. Aquino, Int. J. Quantum Chem. **54**, 107 (1995).
 - [31] Á. Nagy and K. D. Sen, J. Chem. Phys. **115**, 6300 (2001); K. D. Sen and H. E. Montgomery, Jr., Int. J. Quantum Chem. (to be published).
 - [32] C. Schwartz, J. Math. Phys. **26**, 41 (1985).